Physics – Uspekhi **49** (9) 937 – 946 (2006) ©2006 Uspekhi Fizicheskikh Nauk, Russian Academy of Sciences

METHODOLOGICAL NOTES PACS numbers: **01.50.–i**, 41.20.Gz

Braking of a magnetic dipole moving with an arbitrary velocity through a conducting pipe

B A Knyazev, I A Kotel'nikov, A A Tyutin, V S Cherkassky

DOI: 10.1070/PU2006v049n09ABEH005881

Contents

Abstract. Lectures introducing students to electromagnetic induction phenomena often feature the popular experiment in which a small magnet falling down a long conducting pipe is markedly decelerated by the retarding force due to Foucault eddy currents arising in the pipe. In this paper, a formula for the retarding force, valid both for low velocities (when the force is proportional to the velocity v of magnet motion) and high velocities (when it first decreases as v^{-1} and then as $v^{-1/2}$), is derived. The last two regimes are analogous to the collisionless (and hence unbounded) acceleration of plasma electrons and have not been previously described in the literature. The calculation of the retarding force in the presence of a longitudinal cut in the pipe wall is carried out, and experiments to measure this force are discussed.

1. Introduction

The fall of a magnet down a vertical conducting pipe is a popular and showy experiment used to introduce physics students to electromagnetic induction phenomena. An alternating magnetic flux created by a moving magnet induces eddy currents in the conducting walls of the pipe. These currents give rise to a secondary magnetic field that, in turn, brings about a retarding force. Magnetic braking markedly slows down the fall of a magnet in a metal pipe compared with the velocity of its free fall in a nonconducting pipe. By way of example, a small magnet falls down a 1-m long glass pipe, as described in Section 3 below, in 0.6 s versus 10 s in a copper pipe.

The effect of magnetic braking has been investigated both theoretically and experimentally in many works utilizing conductors of different geometry, such as a flat sheet, magnetic suspension, rotating disk, and pipe [1 – 9]. MacLatchy, Backman, and Bogan [5] expounded the simplest theory of the breaking force acting on a magnet in an infinitely long pipe in proportion to the velocity v of magnet motion. The same authors calculated the terminal magnet velocity v_∞ and experimentally recorded the electromotive force using a coil wound around a copper pipe. Hahn and co-workers [7] studied resonant oscillations of a magnet suspended by a small spring in pipes of different diameter and conductivity. The theory developed by these authors is analogous to the theory described in Refs [3, 5] but takes into consideration the finite pipe length.

The aforementioned experiment with a magnet falling down a conducting pipe in the gravitational field has long been used at Novosibirsk State University as a training aid for undergraduates attending relevant lectures [10]. A few years ago, we reviewed publications on magnetic braking with the goal of extending the range of laboratory works offered to the students. It turned out that the theory of this phenomenon is confined to the point magnetic dipole approximation for simulating a magnet of finite dimensions. Moreover, it considers only weak skin effects when the depth δ (skin depth) of magnetic field penetration into a metal is significantly larger than the pipe wall thickness h and pipe magnetic permeability is unity ($\mu = 1$). The above assumptions are not always valid, giving an incentive to construct a more general theory of magnetic braking.

Analysis of experiments with a falling magnet, described in the literature, showed that some features of this phenomenon remain unexplored. Suffice it to say that, to our knowledge, experimenters have measured only the terminal

B A Knyazev, I A Kotel'nikov G I Budker Institute of Nuclear Physics, Siberian Branch of the Russian Academy of Sciences,
prosp. Lavrent'eva 11, 630090 Novosibirsk, Russian Federation
Tel. (7-383) 339 42 68
E-mail: B.A.Knyazev@inp.nsk.su; i.a.kotelnikov@inp.nsk.su
A A Tyutin, V S Cherkassky Department of Physics, Novosibirsk State University,
ul. Pirogova 2, 630090 Novosibirsk, Russian Federation
Tel. (7-383) 339 78 05
E-mail: cherk@phys.nsu.ru

Received 31 August 2005
Uspekhi Fizicheskikh Nauk **176** (9) 965 – 974 (2006)
Translated by Yu V Morozov; edited by A Radzig

magnet velocity, disregarding deceleration dynamics. Nor have they studied magnet movement in a pipe with cracks and slits. This paper was designed to make up for the lack of relevant theoretical and experimental data.

2. Theory

The general theory expounded in Section 2.3 does not use any preliminary propositions concerning the relationship between the parameters δ and h. Nevertheless, we shall first consider particular cases of weak and strong skin effects, when $\delta/h \gg 1$ and $\delta/h \ll 1$, respectively, and only afterwards shall we proceed to the construction of the general theory. We believe that such an approach is more instructive since it allows for deeper insight into the mechanism of magnetic braking.

For the reader's convenience, Section 2.1 describes the standard deceleration theory applicable at a low velocity of magnet motion. Conversely, Section 2.2 considers the high velocity case and demonstrates that the retarding force decreases with increasing speed in proportion to $v^{-1/2}$. In Section 2.3, the general formula that is valid for the entire velocity range (regardless of relativistic effects) is derived. This formula suggests the existence of an intermediate regime in which the retarding force is proportional to v^{-1}. The concluding theoretical Section 2.4 presents the solution to the magnet motion problem for a nonmagnetic pipe with a long longitudinal cut in the low-velocity approximation.

2.1 Weak skin-effect approximation

The magnetic field of a moving magnet induces eddy currents in the conducting walls of a pipe. If the magnet moves parallel to the pipe axis and its poles are aligned along this axis, the eddy currents flow in the azimuthal direction (Fig. 1a). The induced currents generate a nonuniform 'secondary' magnetic field that acts on the falling magnet with the force

$$\mathbf{F} = (\mathbf{m}\,\nabla)\,\mathbf{B}\,, \tag{1}$$

where $\mathbf{m}$ is the dipole magnetic moment. This force opposes the magnet velocity and therefore slows down the motion. In what follows, we shall consider, for certainty, a magnet falling in the gravitational field, although the nature of the force that causes the magnet to move is not an important issue for calculating magnetic braking force. Because the retarding force grows with increasing velocity, the speed of a magnet falling in the gravitational field eventually becomes constant and gravity and retarding forces counterbalance each other.

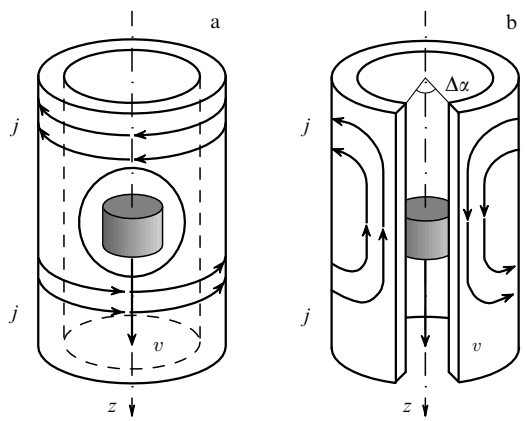

Figure 1. Schematic representation of a magnet falling down a whole (a) and a cut (b) conducting pipe.

As was emphasized in the Introduction, it is usually assumed in the theoretical description of magnetic braking, either explicitly or implicitly, that the pipe slightly perturbs the magnetic field of the moving magnet. Consequently, this field can be calculated as if the magnet were falling in a free space. This assumption holds, first, for a nonmagnetic pipe, and, second, at a relatively low velocity v of motion when the effective skin depth $\delta = c/\sqrt{2\pi\sigma\omega}$, estimated for the characteristic frequency $\omega \sim v/a$ and the given conductivity σ of the wall material, exceeds the pipe radius a. A more accurate criterion will be formulated in Section 2.3.

Our derivation of the retarding force formula in this section resembles that in Ref. [3], but we have modified it so as to create a link with Section 2.2, where the case of strong skin effect is considered.

Let us replace the magnet of a finite size by a point dipole (as in the conventional theory) and suppose that the dipole magnetic moment $\mathbf{m}$ is coaxial with the z-axis of the circular pipe having inner and outer radii a and b, respectively. Let the dipole move along the pipe z-axis corresponding to $r = 0$ in the cylindrical coordinate system (r, α, z) and its position on the z-axis at an arbitrary instant of time t be given by function $z_m(t)$.

The axial symmetry of the problem allows for the choice of such a gauge in which the scalar potential ϕ is everywhere equal to zero, while the vector potential $\mathbf{A}$ has only an azimuthal component: $\mathbf{A} = A_\alpha(r, z, t)\,\mathbf{e}_\alpha$. Then, only the following components of the electromagnetic field have a nonzero value:

$$B_r = -\frac{\partial A_\alpha}{\partial z}\,, \quad B_z = \frac{1}{r}\,\frac{\partial r A_\alpha}{\partial r}\,, \quad E_\alpha = -\frac{1}{c}\,\frac{\partial A_\alpha}{\partial t}\,. \tag{2}$$

In the case of weak skin effect, the magnetic field of the magnet is almost unperturbed by the pipe wall, provided it is made from a nonmagnetic material, i.e., $\mu = 1$. Then, one finds

$$A_\alpha(r, z, t) = \frac{mr}{\left[r^2 + (z - z_m(t))^2\right]^{3/2}}\,. \tag{3}$$

Taking into account that $\partial A_\alpha/\partial t = -v\,\partial A_\alpha/\partial z$, where $v = \dot{z}_m$ is the instantaneous velocity of dipole motion, it is possible to straightforwardly calculate the induced electric field E_α. This field generates an eddy current of density $j_\alpha = \sigma E_\alpha$ in the pipe wall. The current, in turn, establishes a 'secondary' magnetic field that has only a z-component on the z-axis:

$$B_z(z, t) = \frac{1}{c}\int_{-L/2}^{L/2} \mathrm{d}z' \int_a^b \mathrm{d}r'\, \frac{2\pi r'^2\, j_\alpha(r', z')}{\left[r'^2 + (z - z')^2\right]^{3/2}}\,, \tag{4}$$

where $\pm L/2$ are the z-coordinates of the pipe ends. The field gradient at the dipole location point is calculated by differentiating the integrand in formula (4) with respect to z and then equating z to $z_m(t)$. Multiplication of the result by m yields the retarding force

$$F = -\frac{18\pi\sigma m^2 v}{c^2}\int_{-L/2}^{L/2} \mathrm{d}z' \int_a^b \mathrm{d}r'\, \frac{r'^3\,(z_m - z')^2}{\left[r'^2 + (z_m - z')^2\right]^5}\,. \tag{5}$$

The force F is practically independent of the dipole coordinate $z_m(t)$ if the dipole is far enough from the pipe ends. In the

limit $|z_m \pm L/2| \gg a$, Eqn (5) gives

$$F = -\frac{15\pi^2 \sigma m^2 v}{64c^2}\left(\frac{1}{a^3} - \frac{1}{b^3}\right). \tag{6}$$

For a thin-wall pipe, $h = b - a \ll a$ and expression (6) reduces to the well-known result [3]

$$F = -\frac{45\pi^2}{64}\,\frac{\sigma m^2 v\, h}{a^4 c^2}\,. \tag{7}$$

Evidently, the 'minus' sign here indicates that the force is opposite to the magnet velocity and thus justifies its definition as a 'retarding force'.

The braking force can also be computed from the energy balance. Indeed, the power P dissipated in the conducting pipe wall equals (with the opposite sign) the work $A = vF$ done by the retarding force per unit time, namely

$$P = \int_{-L/2}^{L/2} \mathrm{d}z' \int_a^b \mathrm{d}\rho\, 2\pi\, \rho\, \sigma E_\alpha^2(\rho, z')\,.$$

The calculation of the electric field E_α with the help of Eqns (2) and (3) and the division of the resulting P in the limit $L \to \infty$ by $-v$ lead to the same formula (6).

The 'energy balance' method of computation will be used in Section 2.2 where the magnetic braking force is found in the limit of very fast magnet motion.

2.2 Strong skin-effect approximation

Let the velocity of the magnet motion be so high that the skin depth $\delta = c/\sqrt{2\pi\sigma\mu\omega}$, estimated from the characteristic frequency $\omega \sim v/a$, is small compared with the pipe wall thickness h: $\delta \ll h$. Such a high velocity can be attained if the magnet is accelerated using an air rifle or a spring instead of gravity force. For $\delta \ll h$, the magnetic flux is 'squeezed' inside the pipe and eddy currents substantially weaken the magnetic field outside the pipe even if the magnetic permeability μ is close to unity and the magnetic (static) screening has no appreciable effect.

Because the motion of a macroscopic magnet in any case remains pre-relativistic, $v \ll c$, the magnetic field is still possible to calculate in the framework of the quasistatic approximation analogous to that used in Section 2.1. This means that the vector-potential $A_\alpha(r, z, t)$ depends on time t only via the combination $z - vt$, i.e., $A_\alpha(r, z, t) = A_\alpha(r, z - vt)$, provided the dipole is far enough from the pipe ends. Then, one obtains $E_\alpha = (v/c)\,\partial A_\alpha/\partial z$.

Let us assume for the beginning that conductivity of the pipe material is infinitely high, $\sigma = \infty$; consequently, the depth of the magnet field penetration into the pipe walls is negligibly small, i.e., $\delta = 0$. Then, $\mathbf{E} = \mathbf{B} = 0$ both inside and outside the pipe walls. On these assumptions, the corresponding solution of the Maxwell equations for the pipe cavity must satisfy the boundary conditions $E_\alpha = B_r = 0$ at the inner pipe radius, i.e., at $r = a$. For $r < a$, the vector-potential inside the pipe obeys the equation

$$\frac{\partial}{\partial r}\,\frac{1}{r}\,\frac{\partial}{\partial r}\, rA_\alpha + \frac{\partial^2}{\partial z^2} A_\alpha = 0\,, \tag{8}$$

which follows from the equation $\operatorname{rot}\mathbf{B} = 0$ for the static magnetic field. Equation (8) has linearly independent specific solutions in the form $I_1(|kr|)\exp(\mathrm{i}kz)$ and $K_1(|kr|)\exp(\mathrm{i}kz)$, where I_m and K_m are the Bessel functions of order m of imaginary arguments of the first and second kinds, respectively [11]. Therefore, the vector-potential at $r < a$ may be written in the form of the Fourier integral

$$A_\alpha = \frac{2m}{\pi}\int_0^\infty \mathrm{d}k\, k\, \cos(kz - kvt)\left[K_1(kr) + \alpha_k I_1(kr)\right]. \tag{9}$$

The first term in the square brackets under the integral sign is singular at the magnetic dipole location point. Because one has

$$\frac{r}{(r^2 + z^2)^{3/2}} = \frac{2}{\pi}\int_0^\infty \mathrm{d}k\, k\, \cos(kz)\, K_1(kr)\,,$$

this term describes the magnetic dipole potential in a free space. The second term in the square brackets in Eqn (9) is regular, and coefficients α_k can be found from the boundary conditions $A_\alpha = 0$ at $r = a$:

$$\alpha_k = -\frac{K_1(ka)}{I_1(ka)}\,.$$

Now, the magnetic braking force can be found by simply computing the total power P dissipated in the pipe wall and equating this power to the work $-vF$ done by the retarding force F per unit time. The total dissipated power is equal to the energy flux

$$P = 2\pi\int_{-\infty}^{\infty} S_r\, \mathrm{d}z \tag{10}$$

across the inner pipe-wall surface, where $S_r = (c/4\pi)\, E_\alpha B_z$ is the radial component of the Poynting vector at $r = a$. We have chosen infinite integration limits in formula (10), thus neglecting end effects. However, the direct calculation indicates that in the approximation employed $P = 0$, because $E_\alpha = 0$ at $r = a$, meaning the absence of energy flow towards the pipe wall. In other words, the magnetic braking force is negligibly small in the limit $\sigma \to \infty$, as common sense dictates. On the other hand, the disappearance of the retarding force is in conflict with the result from Section 2.1 which, for this reason, proves valid only at slow motions or poor conductivity of the pipe material.

The calculation of the electromagnetic field of a moving magnet at a high but finite pipe conductivity is a difficult task (see Section 2.3). For all the seeming idleness of the calculations presented in a previous paragraph for the case of $\sigma = \infty$, they make it possible to find the magnetic braking force in the limit of a large but finite conductivity, if the Leontovich boundary condition [12] at the inner wall surface is used to express the electric field E_α through B_z. According to Leontovich, the amplitude of the Fourier image of an electric field:

$$E_{\alpha\omega} = \int_{-\infty}^{\infty} E_\alpha\, \exp(\mathrm{i}\omega t)\, \mathrm{d}t$$

is equal to the Fourier image of a magnetic field, namely

$$B_{z\omega} = \int_{-\infty}^{\infty} B_z\, \exp(\mathrm{i}\omega t)\, \mathrm{d}t\,,$$

multiplied by the surface impedance:

$$E_{\alpha\omega} = \left[1 - \operatorname{sign}(\omega)\right]\sqrt{\frac{\mu|\omega|}{8\pi\sigma}}\, B_{z\omega}\,. \tag{11}$$

Because the longitudinal magnetic field

$$B_z = -\frac{2m}{\pi}\int_0^\infty \frac{\mathrm{d}k\,k}{aI_1(ka)}\cos(kz - kz_m)$$

at the pipe surface at $r = a$ does not disappear even in the limit $\sigma \to \infty$, it can be used to calculate the Fourier amplitude

$$B_{z\omega} = -\frac{2m|\omega/v|}{a\,vI_1(|\omega a/v|)}\exp\left(-\frac{\mathrm{i}\omega z}{v}\right), \tag{12}$$

and thereafter to find the electric field at the wall surface with a finite conductivity by means of Eqn (11). Parseval's theorem makes it easy to express the ohmic loss power in the pipe wall through $B_{z\omega}$:

$$P = \frac{acv}{2\pi}\int_0^\infty \mathrm{d}\omega\,\sqrt{\frac{\mu\omega}{8\pi\sigma}}\,\left|B_{z\omega}\right|^2 .$$

Integration and division of P by $-v$ gives the magnetic braking force in the strong skin-effect limit:

$$F = -\frac{m^2c\sqrt{\mu}}{\sqrt{2\pi^3 v\sigma a^9}}\int_0^\infty \mathrm{d}\xi\,\frac{\xi^{5/2}}{I_1^2(\xi)} = -\frac{3.45\,m^2c\sqrt{\mu}}{\sqrt{4\pi\,v\sigma a^9}} . \tag{13}$$

The force F decreasing with the growth in v in proportion to $v^{-1/2}$, the magnet motion proves unstable because an occasional rise in velocity leads to unlimited acceleration. Such a phenomenon is known from plasma physics where suprathermal electrons are unrestrictedly accelerated by the external electric field as the consequence of a decrease in the friction force proportional to the cube of their velocity. In Section 2.3, the existence of an additional, intermediate regime will be demonstrated, in which $F \propto v^{-1}$ in the interval of $1 \ll \delta/h \ll a/\mu\delta$.

2.3 Exact solution

The slightly modified method used in Section 2.2 makes it possible to calculate magnetic braking force in the entire range of possible magnet velocities. To this effect, Eqn (9) should be advantageously rewritten in the form

$$A_\alpha(r, z - vt) = \frac{m}{\pi}\int_{-\infty}^{\infty} \mathrm{d}k\,\exp\left[\mathrm{i}k(z - vt)\right]|\,k\,| \times \left[K_1\left(|\,kr\,|\right) + \alpha_k\,I_1\left(|\,kr\,|\right)\right] ,$$

on the assumption that the coefficient α_k can acquire complex values inside the pipe, i.e., for $r < a$. A similar expression should be written for other space regions, too, because in the general case it may not be reckoned *a priori* that the field is close to the magnetic dipole field, as in the case of weak skin effect, or vanishes, as in the case of strong skin effect.

In the region $r > b$ outside the pipe, the Fourier integral must contain only terms decreasing as $r \to \infty$:

$$A_\alpha(r, z - vt) = \frac{m}{\pi}\int_{-\infty}^{\infty} \mathrm{d}k\,\exp\left[\mathrm{i}k(z - vt)\right]\beta_k\,|\,k\,|\,K_1\left(|\,kr\,|\right). \tag{15}$$

The vector-potential inside the conducting pipe walls, for $a < r < b$, satisfies the equation

$$\frac{\partial}{\partial r}\,\frac{1}{r}\,\frac{\partial}{\partial r}\,rA_\alpha + \frac{\partial^2}{\partial z^2}\,A_\alpha = -\frac{4\pi\sigma\mu}{c^2}\,\frac{\partial A_\alpha}{\partial t} , \tag{16}$$

as follows from equations $\mathrm{rot}\,\mathbf{H} = 4\pi\mathbf{j}/c$, $\mathrm{rot}\,\mathbf{E} = -(1/c)(\partial/\partial t)\,\mathbf{B}$, $\mathbf{j} = \sigma\mathbf{E}$, and $\mathbf{B} = \mu\mathbf{H}$. The relevant solution of Eqn (16) may be written down in the form

$$A_\alpha(r, z) = \frac{m}{\pi}\int_{-\infty}^{\infty} \mathrm{d}k\,\exp\left[\mathrm{i}k(z - vt)\right]|\,k\,| \times \left[\mu_k I_1(\varkappa r) + \nu_k\,K_1(\varkappa r)\right] , \tag{17}$$

where $\varkappa = \sqrt{k^2 - 4\pi\mathrm{i}kv\sigma\mu/c^2}$.

Coefficients α_k, β_k, μ_k, and ν_k must be found from the boundary conditions at the inner and outer wall surfaces. These conditions include the continuity of the vector potential A_α and its derivative $\partial A_\alpha/\partial r$ at $r = a$ and $r = b$. The magnetic braking force can be calculated knowing only the coefficients α_k, because

$$F = \frac{m^2}{\pi}\int_0^\infty \mathrm{d}k\,\mathrm{i}k^3\left[\alpha_k - \alpha_{-k}\right] . \tag{18}$$

Simple but cumbersome calculations yield

$$\alpha_k = -\frac{K_+(a)\,K_-(b) - K_-(a)\,K_+(b)}{I_-(a)\,K_-(b) - I_+(a)\,K_+(b)} , \tag{19}$$

where

$$K_+(r) = \varkappa I_0(\varkappa r)\,K_1\left(|\,k\,|r\right) + \mu|\,k\,|\,I_1(\varkappa r)\,K_0\left(|\,k\,|r\right) ,$$

$$K_-(r) = \varkappa K_0(\varkappa r)\,K_1\left(|\,k\,|r\right) - \mu|\,k\,|\,K_1(\varkappa r)\,K_0\left(|\,k\,|r\right) ,$$

$$I_+(r) = \varkappa K_0(\varkappa r)\,I_1\left(|\,k\,|r\right) + \mu|\,k\,|\,K_1(\varkappa r)\,I_0\left(|\,k\,|r\right) ,$$

$$I_-(r) = \varkappa I_0(\varkappa r)\,I_1\left(|\,k\,|r\right) - \mu|\,k\,|\,I_1(\varkappa r)\,I_0\left(|\,k\,|r\right) .$$

The results of Sections 2.1, 2.2 [expressions (6) and (13)] can be derived from the general solution (18) in the corresponding limiting cases even though the passage to the limit proves to be a nontrivial problem.

In order to obtain new results unrepresented earlier, the friction force (18) should be written down in the parametric form

$$F = -\frac{m^2}{a^4}\,\mathcal{F}(\mu, \varepsilon, \eta) , \tag{20}$$

where function $\mathcal{F}$ depends on three dimensionless parameters: μ, $\varepsilon = (b - a)/a$, and $\eta = 4\pi\sigma va/c^2$.

In the case of $\eta \ll 1$, corresponding to the small velocity limit considered in Section 2.2 under the additional condition $\mu = 1$, the general formula (18) can be reduced to a visually graspable expression at an arbitrary value of μ if the pipe wall is sufficiently thick, i.e., for $\varepsilon \gg 1$:

$$\mathcal{F} = \frac{\eta}{\pi}\int_0^\infty \mathrm{d}x\,\frac{\mu^2x^4\left[K_2(x)\,K_0(x) - K_1^2(x)\right]}{\left[1 + (\mu - 1)\,xI_0(x)\,K_1(x)\right]^2} . \tag{21}$$

Function (21) is given in Fig. 2.

At $\mu = 1$, integration in formula (21) yields

$$\mathcal{F} = \frac{15\pi}{256}\,\eta \approx 0.184\,\eta \tag{22}$$

in agreement with formula (6). At large μ, function (21) tends to almost twice this value:

$$\mathcal{F} \approx 0.359\,\eta . \tag{23}$$

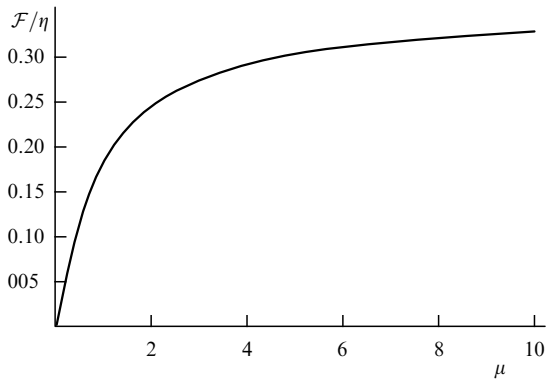

Figure 2. Function $\mathcal{F}$ plotted versus μ for $\eta \ll 1$.

For $\varepsilon \ll 1$, it is possible to use the results of Section 2.1, because formula (7) is valid at any μ and does not depend on it. In dimensionless variables, Eqn (7) assumes the form

$$\mathcal{F} = \frac{45\pi}{256}\,\varepsilon\eta \approx 0.552\,\varepsilon\eta\,. \tag{24}$$

Evidently, the friction force is not very sensitive to the magnetic properties of the pipe when the motion is slow. However, this assertion is true only if the magnet moves exactly along the axis of a cylindrical pipe. Any deviation from the axis would cause attraction and, possibly, attachment of the magnet to the ferromagnetic wall of the pipe.

The opposite case of vast motion, considered in Section 2.2, takes place for $\varepsilon\eta \gg 1/(\mu\varepsilon)$. Then, one arrives at

$$\mathcal{F} = \frac{\sqrt{2\mu}}{\pi\sqrt{\eta}} \int_0^\infty \frac{\mathrm{d}\xi\,\xi^{5/2}}{I_1^2(\xi)} \approx 3.45\sqrt{\frac{\mu}{\eta}}, \tag{25}$$

in conformity with Eqn (13).

There is an intermediate interval $1 \ll \varepsilon\eta \ll 1/(\mu\varepsilon)$ between the limiting cases (24) and (25), on which the friction force is proportional to v^{-1}:

$$\mathcal{F} = \frac{2}{\pi\varepsilon\eta} \int_0^\infty \frac{\mathrm{d}\xi\,\xi^2}{I_1^2(\xi)} \approx \frac{4.78}{\varepsilon\eta}\,. \tag{26}$$

The interval exists if $\varepsilon \ll 1/\mu$ and corresponds to the case where the thickness of the pipe wall, $h = b - a$, is smaller than that of the skin depth, δ, but exceeds a certain value, namely, $\delta^2\mu/a \ll h \ll \delta$. In this parameter interval, the conducting cylinder effectively screens the electromagnetic field even if $\delta \gg h$ [13, 14].

Figure 3 illustrates the possibility of realizing regimes (25) and (26) for various materials. For a copper pipe with a relative wall thickness $h/a = 0.25$, the dependence $F \propto v^{-1/2}$ is realized when $va \sim 10^4$ cm^2 s^{-1}, and $F \propto v$ when $va \sim 2\times10^3$ cm^2 s^{-1}; at $a = 0.665$ cm, the corresponding magnet velocities should be 200 and 40 m s^{-1}, respectively. For a thick pipe of copper with a wall thickness $h = 2.5$ mm and a mean radius $R = (a+b)/2 = 4$ mm, the required magnet velocities are 40 and 6 m s^{-1}, respectively. Such values are attainable in a simple student experiment.

The entire range $\varepsilon\eta \ll 1/(\mu\varepsilon)$ is described by the formula

$$\mathcal{F} = \frac{2\varepsilon\eta}{\pi} \int_0^\infty \frac{\mathrm{d}\xi\,\xi^4 K_1^2(\xi)}{1 + \varepsilon^2\eta^2\xi^2 I_1^2(\xi)\,K_1^2(\xi)}\,. \tag{27}$$

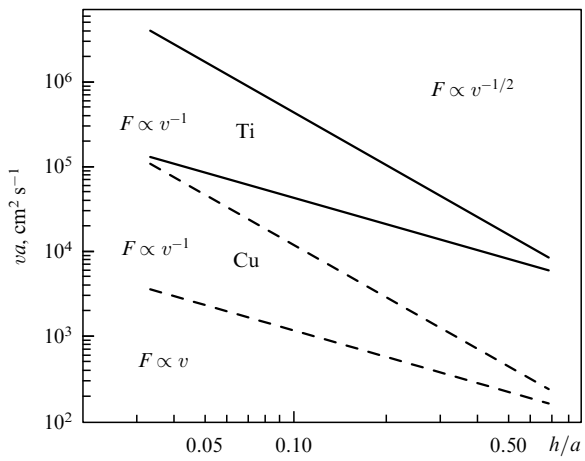

Figure 3. Regions with different functional dependences $F(v)$. The regions between the straight lines of each set (solid for a titanium pipe, and dashed for a copper one) correspond to the dependences $F \propto v^{-1}$; $F \propto v$ in the region below the bottom line, and $F \propto v^{-1/2}$ in the region above the top line.

Formula (27) can be derived from the 'first principles' if the change of A_α over the pipe wall thickness (i.e., a change in the electric field and current density) is neglected. In such a case, the pipe wall may be represented in the form of an infinitely thin current layer and the solutions (14) and (15) inside and outside the pipe, respectively, matched the help of the boundary conditions $E_\alpha(a+0) - E_\alpha(a-0) = 0$ and $B_z(a+0) - B_z(a-0) = -4\pi I/c$, where $I = \sigma h E_\alpha(a)$ is the total current per unit length of a pipe wall. Function (27) is independent of μ (Fig. 4). Therefore, the magnetic braking force in a thin-walled pipe, $\varepsilon \ll 1$, does not depend on the magnetic properties of its material, while the dependence on other parameters ε and η is expressed only through their product if $\varepsilon\eta \ll 1$. This force reaches a maximum value, $\mathcal{F} = 0.704$, at $\varepsilon\eta = 2.69$.

In what follows, the comparison of the above results with experimental data will be confined to the case described by formula (27) on the assumption that $\varepsilon \ll 1$ and $\varepsilon\eta \ll 1/(\mu\varepsilon)$. In dimensional units, these inequalities are converted to the forms $h \ll a$ and $h \ll \delta$, respectively, where $\delta \sim c/\sqrt{2\pi\sigma\mu v/a}$.

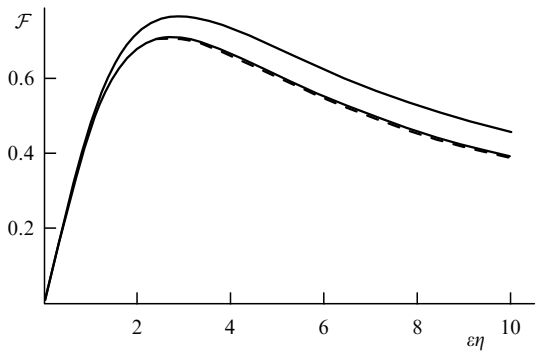

Figure 4. The magnetic braking force for a thin conducting wall. The dashed line corresponds to the approximate solution (27) that holds when $\varepsilon\eta \ll 1/(\mu\varepsilon)$ in the limit $\varepsilon \to 0$. Solid lines show the exact solution at $\mu = 1$ for two values of ε: $\varepsilon = 0.1$ (upper curve), and $\varepsilon = 0.01$ (closely coinciding with the dashed line).

2.4 Pipe with a longitudinal cut

A longitudinal cut interrupts the azimuthal current circulating through the a pipe wall. However, there exist at least two effects maintaining the current.

The first one is the displacement current $-(1/c)\,\partial\mathbf{E}/\partial t$, which is able, in principle, to 'intercept' the conduction current at slit edges, but this effect is insignificant at small velocities.

The second effect is more important. Because eddy currents induced by an electromotive force flow in opposite directions in front of and behind a moving magnet (see Fig. 1), they may close at the slit edges. In the quasistatic approximation, the electric charge cannot accumulate in the wall bulk spreading over the wall surface so as to ensure that the conduction currents are closed. In the wall bulk, one has

$$\mathbf{E} = \frac{v}{c}\,\frac{\partial A_\alpha}{\partial z}\,\mathbf{e}_\alpha - \nabla\phi\,, \tag{28}$$

where $A_\alpha = mr/[r^2 + (z - vt)^2]^{3/2}$ is the vector-potential of the point magnetic dipole m in a free space, and ϕ is the scalar (electric) potential induced by surface charges; approximation (28) corresponds to the case of weak skin effect.

Potential ϕ satisfies the Laplace equation $\Delta\phi = 0$ inside the wall. The Laplace equation for a thin wall ($h \ll a$) can be simplified taking into consideration the absence of the radial electric field inside the wall: $\partial\phi/\partial r = 0$. Then, only the derivatives with respect to α and z are retained in the Laplace equation which takes the following form if variable r is substituted by the pipe radius a:

$$\frac{1}{a^2}\,\frac{\partial^2\phi}{\partial\alpha^2} + \frac{\partial^2\phi}{\partial z^2} = 0\,. \tag{29}$$

The absence of the radial electric field ensues from the boundary conditions for the current density

$$\mathbf{j} = \sigma\mathbf{E} \tag{30}$$

that must disappear at the boundary of the conducting material if the displacement current is negligible. The solution of Eqn (29) is sought in the form

$$\phi(\alpha, z) = \int_0^\infty \mathrm{d}k\,\sin(kz - kvt) \times \left[\mu_k \exp(ka\alpha) + \nu_k \exp(-ka\alpha)\right], \tag{31}$$

and the coefficients μ_k, ν_k are found from the boundary conditions for the azimuthal component of the current density, $j_\alpha = 0$, at both slit edges.

By denoting the angular width of the slit with $\Delta\alpha$ (see Fig. 1) and assuming that its edges correspond to azimuths $\alpha = \pm(\pi - \Delta\alpha/2)$, one arrives at

$$\mu_k = -\nu_k = -\frac{mv}{\pi c}\,\frac{kK_1(ka)}{\cosh\left[(\pi - \Delta\alpha/2)ka\right]}\,. \tag{32}$$

The power dissipated in the wall is equal to

$$P = h\int_{-\pi+\Delta\alpha/2}^{\pi-\Delta\alpha/2} \mathrm{d}\alpha\, a \int_{-\infty}^{\infty} \mathrm{d}z\,\frac{j_\alpha^2 + j_z^2}{\sigma}\,, \tag{33}$$

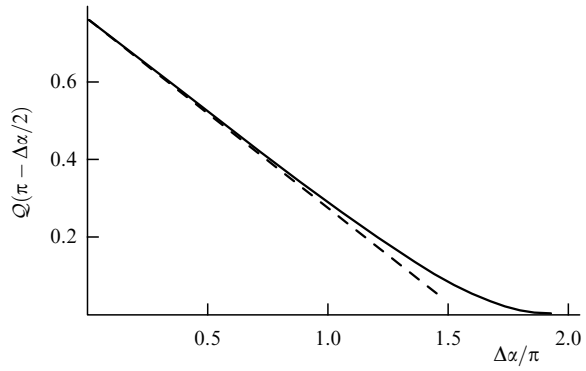

Figure 5. Function $\mathcal{Q}(\pi - \Delta\alpha/2)$ (solid curve) and its linear approximation (dashed straight line).

where the current density components j_α, j_z are calculated with the help of equations (28) and (30)–(32):

$$j_\alpha = \frac{2m\sigma v}{\pi c}\int_0^\infty \mathrm{d}k\,k^2\,K_1(ka)\,\sin\left[k(z - vt)\right] \times \frac{\cosh[ka\alpha] - \cosh\left[(\pi - \Delta\alpha/2)\,ka\right]}{\cosh[(\pi - \Delta\alpha/2)\,ka]}\,,$$
$$j_z = \frac{2m\sigma v}{\pi c}\int_0^\infty \mathrm{d}k\,k^2\,K_1(ka)\,\cos\left[k(z - vt)\right] \times \frac{\sinh[ka\alpha]}{\cosh\left[(\pi - \Delta\alpha/2)\,ka\right]}\,. \tag{34}$$

Integration over z and α in Eqn (33) and division of the result by $-v$ yields the magnetic braking force

$$\mathcal{F} = -\frac{45\pi}{256}\,\mathcal{Q}\left(\pi - \frac{\Delta\alpha}{2}\right)\varepsilon\eta\,, \tag{35}$$

where the function

$$\mathcal{Q}(\beta) = \frac{512}{45\pi^3}\int_0^\infty \mathrm{d}\xi\,\xi^3 K_1^2(\xi)\left[\beta\xi - \tanh(\beta\xi)\right]$$

gives the ratio of the retarding forces in slit and unslit pipes (Fig. 5). For $\Delta\alpha \leqslant 3\pi/2$, this dependence can be approximated to within a few percent by the linear function

$$\mathcal{Q}\left(\pi - \frac{\Delta\alpha}{2}\right) \approx 0.77 - 0.16\Delta\alpha\,. \tag{36}$$

3. Experiment

We have studied the fall of a magnet in a vertical pipe in the gravitational field. The experimental conditions corresponded to the low-speed motion regime, $\eta \ll 1$. The experimental setup consisted of a few vertical pipes of length $L = 90$ cm, made from copper, aluminium alloy, brass, titanium, and glass. The pipes at hand were not certified and the exact values of their conductivities were unknown. The pipe dimensions are presented in the table. The cylindrical magnet of a neodymium/iron/boron alloy 1 cm in diameter and 1 cm in length was magnetized along the axis. The magnet started to fall from the upper pipe end with a zero velocity. Seven coils were wound around the outer surface of each pipe with a period of 10 cm. Each coil contained 20 turns and was

Table. Pipe characteristics (outer and inner diameters $2a$ and $2b$, aperture angle $\Delta\alpha$, specific conductivity σ) and the main experimental results.

	Copper		Aluminium		Brass	Titanium	Glass
$\Delta\alpha$, rad	—	—	0.32	$\pi/4$	—	—	—
$2a$, mm	11.6	12.4	12.4	12.4	11.7	11.9	11.8
$2b$, mm	15.0	16.0	16.0	16.0	13.9	14.3	15.0
σ, $10^{17}\times\mathrm{s}^{-1}$	5.27	1.74			1.35	0.192	—
β, s^{-1}	143.0	38.0	31.3	23.0	27.2	3.8	0.137
v_1 (v_∞), $\mathrm{cm\,s}^{-1}$	**6.85**	**25.8**	**31.3**	**42.6**	**36.1**	116.0	140.1
m_t, $\mathrm{g}^{1/2}\,\mathrm{cm}^{5/2}\,\mathrm{s}^{-1}$	474 ± 2	—	—	—	—	465 ± 5	—
m_U, $\mathrm{g}^{1/2}\,\mathrm{cm}^{5/2}\,\mathrm{s}^{-1}$	433	429	—	—	425	436	429

Note: The values of σ for copper and titanium are borrowed from the literature, and those for aluminium alloy and brass calculated from Eqn (39). Friction coefficient β, initial magnet velocity v_1 at the level of the first measuring coil, and magnetic moment m_t are found by the least square method, with the time dependence of the distance covered by the magnet being fitted using Eqn (38). The values of v_1 equivalent to the terminal velocity v_∞ are printed in bold. The magnetic moment m_U is obtained by fitting experimental oscillograms to the theoretical ones (40).

as long as 8 mm. The coils were connected together in series and connected to a Tektronix TDS-220 oscillograph.

3.1 Fall of a magnet in a whole pipe

The time dependences of coil voltage for titanium and aluminium pipes are depicted in Fig 6. It is clear that the signals are proportional to the eddy current flowing over the outer pipe surface. The peaks on the oscillograms are in all probability due to the action of the electromotive force in the coil closest to the instantaneous position of the falling magnet. When the magnet moves through the center of the coil, one has $U(t) = 0$; therefore, the time necessary to cover the distance between the neighboring coils can be determined from the oscillogram. The result of such processing is given in Fig. 7, where $t = 0$ corresponds to the beginning of the flight past the upper measuring coil. The $t{-}z$ dependence was constructed over the average values obtained in 12 and more experiments for each pipe. The measurement errors were significantly smaller than the point sizes shown in the plots. In the copper pipe having the highest conductivity, the magnet dropped 70 cm in approximately 10 s. Such a slow drop produced a strong impression, when the experiment was demonstrated to an audience. The electric conductivity of the titanium pipe was 20 times lower, and, accordingly, the time of the magnet's drop was only 0.35 s.

The skin depth δ estimated from the characteristic frequency $\omega \sim v/a$ for all the pipes falls within 4 and 6 cm. This fact justifies the use of the weak skin-effect approxima-

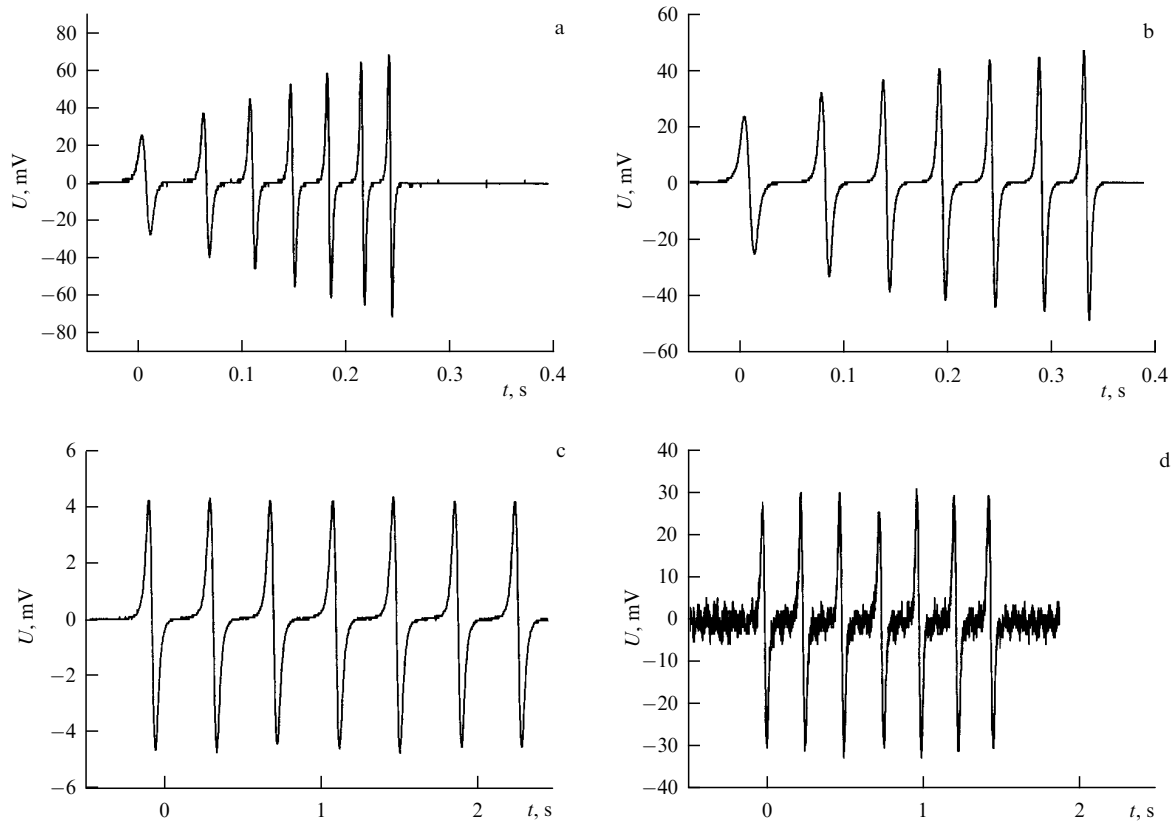

Figure 6. Voltage induced in a series of measuring coils in pipes of (a) glass, (b) titanium, (c) aluminium alloy, and (d) aluminium alloy with a longitudinal cut at $\Delta\alpha = \pi/2$. A series of seven coils was wound around each pipe with a period of 10 cm. Oscillograms for copper, brass, and aluminium ($\Delta\alpha = 0.32$) pipes are analogous to oscillograms (c) and (d).

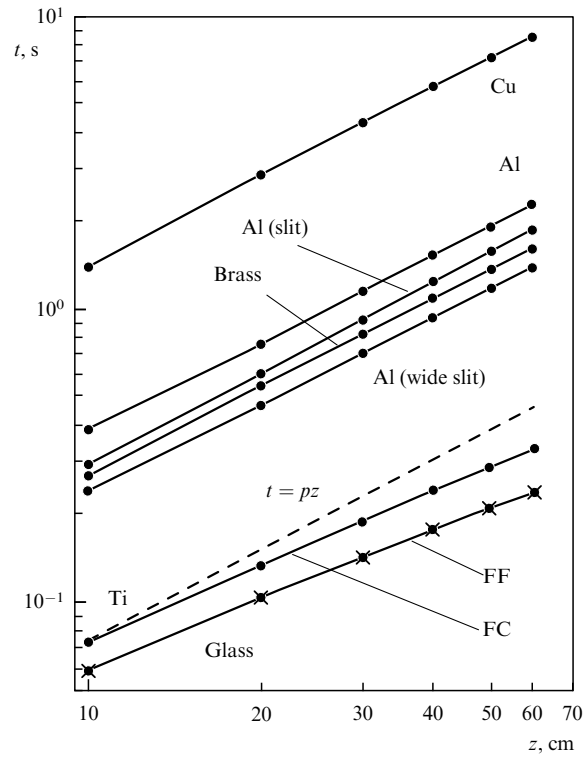

Figure 7. Time of flight as a function of coordinates of the measuring coils. Full circles mark the instants of the magnet's flight through the center of the corresponding coil. Solid lines are theoretical trajectories (14) used to choose the friction coefficient β and the initial velocity v_1. Curve FF for glass is fairly consistent with a free fall. The remaining curves correspond to motion with a constant velocity except curve FC for the titanium pipe, which characterizes the transient regime of magnet acceleration. (Here, p is a certain constant.)

tion in the calculations that follow. The magnetic braking force is proportional to the velocity and may be written down in the form $F = -\beta M \dot{z}_m$, where β is the coefficient of magnetic friction, $M = 5.5$ g is the magnet mass, and $z_m(t)$ is the instantaneous magnet coordinate. The solution to the equation of motion of a magnet:

$$\ddot{z}_m(t) + \beta \dot{z}_m(t) = g \tag{37}$$

in the gravitational field, taking into account the above retarding force at the initial conditions $z_m(0) = 0$, $\dot{z}_m(0) = v_1$, gives

$$z_m(t) = \frac{gt}{\beta} - \frac{g - \beta v_1}{\beta^2}\left[1 - \exp(-\beta t)\right], \tag{38}$$

where v_1 is the magnet velocity at the center of the first coil.

We have used Eqn (38) for fitting the experimental data presented in Fig. 7. They all corresponded to the straight line $t = z/v_\infty$, with the exception of the titanium and glass pipes, because the magnet in a well-conducting pipe reached the terminal velocity $v_\infty = g/\beta$ before flying up to the first measuring coil; for such pipes, one obtains $v_1 = v_\infty$. The magnet freely fell in the glass pipe as indicated by the fitting curve FF (see Fig. 7). The curve FC for the titanium pipe corresponded to the intermediate case where each term in Eqn (37) was equally important.

Knowing the coefficient of friction β and pipe conductivity, it is easy to calculate the magnetic dipole moment with the help of formula (7):

$$m_t = \sqrt{\frac{64\beta M R^4 c^2}{45\pi^2 \sigma h}}, \tag{39}$$

where $R = (a + b)/2$. We have chosen from the data on conductivity available in the literature the following results: $\sigma = (5.27 \pm 0.03) \times 10^{17}$ s^{-1} for copper, and $\sigma = (1.92 \pm 0.04) \times 10^{16}$ s^{-1} for titanium. The calculated values of the magnetic moment m_t are presented in the table. The values of m_t obtained in experiments with copper and titanium pipes reasonably agree with each other. However, statistical variance of the computed value is significantly smaller than the uncertainty in the conductivity values used.

Substituting the thus found mean value of the magnetic moment $\langle m_t \rangle = 469.5 \pm 5.5$ g$^{1/2}$ cm$^{5/2}$ s^{-1} into formula (39), we have calculated conductivity for other pipes without slits. The values obtained, $\sigma = 1.35 \times 10^{17}$ s^{-1} for brass, and $\sigma = 1.74 \times 10^{17}$ s^{-1} for aluminium alloy, lie within the scatter range of the table data cited in different reference books.

The last line in the table contains values of the magnetic moment m_U computed in a different way. In this method, experimental oscillograms were approximated by the formula

$$U(t) = \frac{6\pi m \rho}{c}\, \dot{z}_m(t) \sum_{i=1}^{7} \sum_{j=1}^{20} \frac{\rho\big(z_m(t) - z_{ij}\big)}{\left[\big(z_m(t) - z_{ij}\big)^2 + \rho^2\right]^{5/2}}, \tag{40}$$

where $\rho = b + d/2$ is the radius of the measuring coil turn, d is the wire diameter, z_{ij} is the coordinate of the j turn in the measuring coil number i, and $z_m(t)$ is the magnet coordinate at the instant of time t calculated by formula (38). Summation in expression (40) is over all seven coils and 20 turns in each of them. For the given dependence $z_m(t)$, voltage (40) in the system of coils has the sole fitting parameter m, making the fitting procedure easier because knowledge of material conductivity is not required. Adjustment by the least square method gives very similar values of m_U for all pipes outlined in the table, from a copper pipe to a glass one. However, the mean value of $\langle m_U \rangle$ is 10% smaller than $\langle m_t \rangle$. The former (m_U) appears more reliable than the latter (m_t) because the second method relies on a minimum of additional assumptions and yields a result independent of magnetic braking efficiency. This result is the same for both good conductors, such as copper, and good insulators (e.g., glass).

3.2 Fall of a magnet in a pipe with a longitudinal cut

A longitudinal crack or split in the pipe drastically alters the distribution of eddy currents in the wall. It is shown in Section 2.4 that eddy currents in a well of a slit pipe are closed along the slit edges (Fig. 1b), whereas they form separate lines above and below the magnet in a whole pipe (Fig. 1a). The cut enhances effective pipe resistance, leading to a decrease in the magnetic braking force. When Eqns (35) and (36) are used, the coefficient of friction β for pipes made of aluminium alloy with a narrow ($\Delta\alpha = 0.32$) or wide ($\Delta\alpha = \pi/4$) slit must be $\beta_{\rm th} = 27.6$ s^{-1} and $\beta_{\rm th} = 20.4$ s^{-1}, respectively. The experimental values presented in the table are 10 – 15% higher.

A simple explanation of the discrepancy between theory and experiment can be 'heard' in a literal sense. When a magnet is thrown into a pipe with a slit, a characteristic gritting sound that is absent in an uncut pipe is heard. This means that the magnet rubs against the inner wall if the pipe is cut in its surface but does not touch the wall of the whole pipe. Because the slit breaks the azimuthal symmetry of the pipe,

eddy currents flowing along the opposite sides of the slit establish a magnetic field $\mathbf{B}_\perp$ directed toward it at the instantaneous magnet location point. This field creates a torque moment $\mathbf{K} = \mathbf{m} \times \mathbf{B}_\perp$ that turns the magnet in the plane passing through its center and the middle of the slit. In our experiments, the magnet's diameter was only 2 mm smaller than the inner diameter of the pipe. Due to this, the torque pressed the opposite sides of the magnet to the inner wall surface and thus increased the retarding force compared with the one predicted in Eqn (35) by virtue of mechanical friction of the magnet against the pipe wall.

In order to demonstrate this effect, we cut four 12-cm-long slits in an aluminium pipe 110 cm in length that alternated with 12-cm intact sections. The slits had various angular widths $\Delta\alpha/\pi$: 0.2, 0.1, 0.05, and 0.025. Twenty seven measuring coils were evenly distributed along the pipe length with a period of 4 cm. Figure 8 presents a characteristic oscillogram and time dependence of the magnet velocity. The magnet's motion in such a pipe is rather slow and no special instruments are needed to hear the gritting produced by the magnet passing a slit and its disappearance when the magnet flew by the intact sections. The magnet velocity at the end of all uncut sections reaches a maximum (constant) value but does not drop monotonically with decreasing slit width in the sections with slits, as expected from the analysis of formula (35) in which mechanical friction against the wall is disregarded.

The total retarding force in the cut sections is the sum of magnetic braking and mechanical friction against the wall. The nonmonotonic dependence of the measured retarding force is attributable to the nonmonotonic dependence of the moment of forces K on the slit width. Using the solution of Eqns (34) for the current in the pipe wall, we find that

$$K = \frac{m^2}{a^3}\,\frac{45\pi}{256}\,\mathcal{K}\left(\pi - \frac{1}{2}\,\Delta\alpha\right)\varepsilon\eta\,, \tag{41}$$

where

$$\mathcal{K}(\chi) = \frac{512}{45\pi^3}\int_0^\infty \mathrm{d}y\,\frac{y^3}{1+y^2}\,K_1(y)\left[yK_0(y) + K_1(y)\right] \times \left[y\sin\chi - \cos\chi\tanh(\chi y)\right].$$

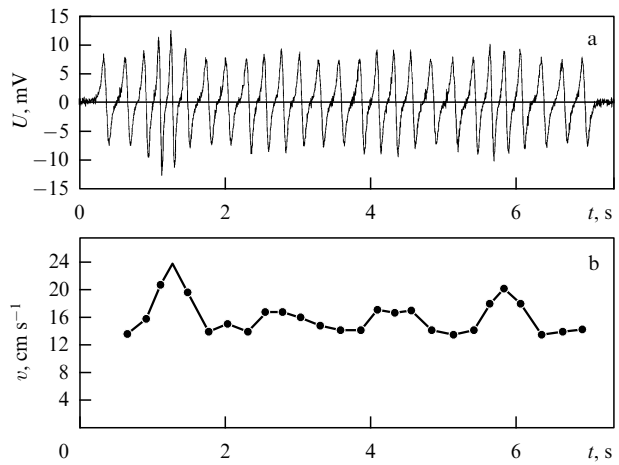

Figure 8. The fall of a magnet in a pipe with a series of longitudinal cuts: (a) oscillograms of the signal from the series of 27 measuring coils, and (b) time dependence of the magnet's velocity computed from the oscillograms. The form of the oscillograms is retained to within a reverse in the time axis direction as the pipe rotates 180° about the horizontal axis.

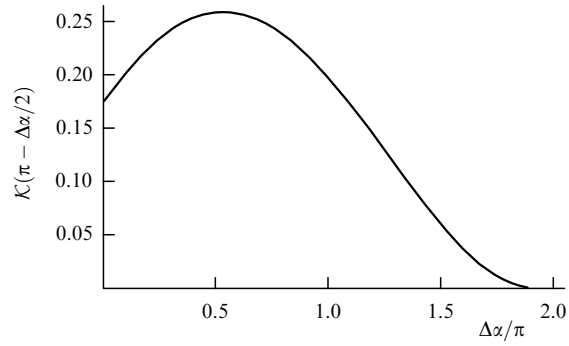

Figure 9. Function $\mathcal{K}(\Delta\alpha)$.

The ratio of the force N of magnet pressure on the wall to the retarding force (24) acting on the magnet in the uncut pipe is proportional to K. The mechanical friction force $F = kN$ is proportional to N, and the coefficient of friction k is usually smaller than unity, $k < 1$. Figure 9 shows that the torque moment reaches its peak at $\Delta\alpha = 0.53\pi = 96°$. The total retarding force can peak at a smaller angular width of the slit, depending on k. This feature qualitatively accounts for the varied magnet velocity observed in experiments with the multiple-slit pipe. Another effect likely to enhance the friction force is an increase in the magnet rotation angle with slit widening.

4. Conclusion

A thorough study of the magnetic braking effect in a conducting pipe turned out to be much more instructive than is commonly believed. We have observed two additional regimes besides the slow motion regime characterized by the linear velocity dependence of the retarding force, in which the force decreases with increasing velocity of motion of a magnet. Such a phenomenon is well known from plasma physics where it leads to a limitless acceleration of electrons in the plasma by the electric field exceeding a critical value.

Our experiments have demonstrated that the deceleration of a magnet may be used to detect cracks in pipe walls. Unexpectedly, the same experiments revealed the nonmonotonic dependence of the retarding force on the slit width that was explained as a result of magnet rotation in the magnetic field of the currents flowing toward the opposite slit edges.

Thus, a simple experiment on magnetic braking may be offered to undergraduate students as a new research topic in a seemingly well-developed field of physics. In particular, the laboratory practicum 'Electricity and Magnetism' at the Department of General Physics, Novosibirsk State University, already includes the course 'Foucault Currents and Magnetic Friction'. More sophisticated experiments may be proposed as the theme of a student's term paper, e.g., verification of our prediction of a regime in which the retarding force decreases with increasing magnet velocity.

Acknowledgments
The authors are grateful to P D Vobly who put the magnet at our disposal, and G V Meledin and A N Matveenko for helpful discussions.

References

1. Marcuso M et al. *Am. J. Phys.* **59** 1118 (1991)
2. Marcuso M et al. *Am. J. Phys.* **59** 1123 (1991)
3. Saslow W M *Am. J. Phys.* **60** 693 (1992)
4. Ribarić M, Šušteršić L *Am. J. Phys.* **60** 513 (1992)
5. MacLatchy C S, Backman P, Bogan L *Am. J. Phys.* **61** 1096 (1993)
6. Cadwell L H *Am. J. Phys.* **64** 917 (1996)
7. Hahn K D et al. *Am. J. Phys.* **66** 1066 (1998)
8. Kraftmakher Y *Eur. J. Phys.* **22** 477 (2001)
9. Redžić D V *Eur. J. Phys.* **23** 127 (2002)
10. Meledin G V, Personal communication (2002)
11. Yahnke E, Emde F, Lösch F *Tafeln Höherer Funktionen* (Stuttgart: Teubner, 1960) [Translated into English: *Tables of Higher Functions* (New York: McGraw-Hill, 1960); [Translated into Russian (Moscow: Nauka, 1964)]
12. Landau L D, Lifshitz E M *Elektrodinamika Sploshnykh Sred* (Electrodynamics of Continuous Media) (Moscow: Nauka, 1982) p. 414 [Translated into English (Oxford: Pergamon Press, 1984)]
13. Fahy S, Kittel C, Louie S G *Am. J. Phys.* **56** 989 (1988)
14. Cherkassky V S, Knyazev B A, Kotelnikov I A "Electromagnetic screening by a thin conducting can", Preprint Budker INP 2003-71 (Novosibirsk: Budker Institute of Nuclear Physics of the Siberian Branch of the Russian Academy of Sciences, 2003)